Seeing the Riemann Zeros in an Antenna Pattern

Brian Scannell

Abstract

The non-trivial zeros of the Riemann zeta function can be made visible as nulls in a simulated antenna radiation pattern. The connection is supplied by a Fourier-transform representation due to van der Pol together with the familiar fact that the far-field pattern of an antenna is the Fourier transform of its aperture field. Starting from this observation, we describe full-wave simulations of two antenna realizations: a prescribed array of dipoles and a more practical electromagnetic realization: a slot array illuminated by a plane wave. The simulated null positions reproduce known Riemann zeros at approximately the percent level, and an extended slot design brings roughly the first eighty-five zeros into the visible range. The construction is not a test of the Riemann Hypothesis; rather, it is a simulated electromagnetic visualization of known zeros on the critical line.

1 Visualising the Riemann zeros

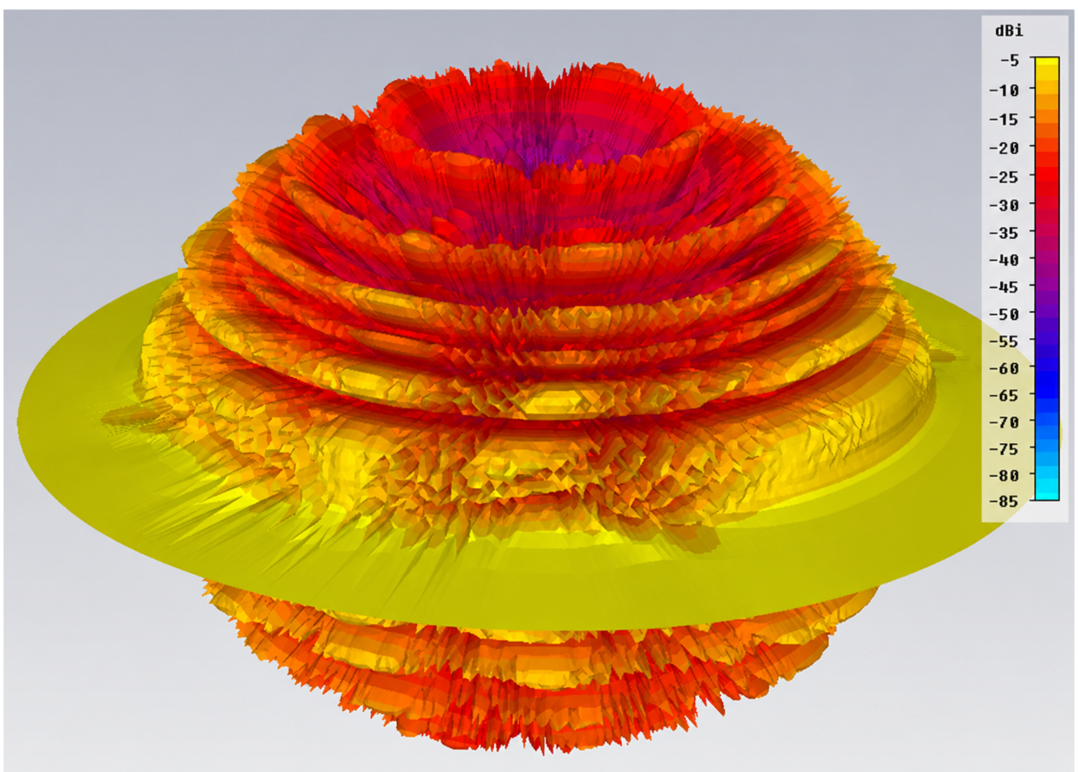

Figure 1: Riemann zeta zeros encoded as nulls in a simulated antenna radiation pattern.

The rippled three-dimensional surface above is a simulated electromagnetic radiation pattern. Hidden within its sequence of nulls are numerical positions corresponding to zeros of the Riemann zeta function.

2 A surprising place to see the zeros

The Riemann zeta function

$$\zeta(s) = \sum_{n=1}^{\infty} \frac{1}{n^s}, \qquad \Re(s) > 1,$$

extends analytically to the complex plane apart from its pole at $s = 1$. Its non-trivial zeros are among the most famous objects in mathematics. Back in 1859, Bernhard Riemann published his only paper on number theory, *On the Number of Prime Numbers Less Than a Given Magnitude* [1]. In just a few pages he posed a conjecture about the zeros of the zeta function that became one of mathematics' most famous unsolved problems and, more than a century later, one of the million-dollar Millennium Prize Problems [2]. Its significance reaches far beyond the 1859 paper: the zeta function is intimately connected with the distribution of the prime numbers that now underpin much of modern public-key cryptography. The Riemann Hypothesis asserts that every non-trivial zero has real part 1/2, so the line

$$s = \frac{1}{2} + it$$

is called the critical line. Nothing in what follows proves or tests that hypothesis. Our aim is different: given zeros already known to lie on the critical line, can one construct a physical system in which their locations appear directly as observable nulls?

The answer comes from an unexpected meeting of number theory and antenna theory. In 1947, van der Pol used an electromechanical method to investigate the zeta function. Much later, Berry showed that propagation into the far field supplies the required Fourier transform and explicitly suggested microwave or radio realization with a suitable antenna. An antenna far field is, to first order in the usual aperture formulation, a Fourier transform of the field across its aperture. If that aperture field is chosen appropriately, the zeros of the transformed field can therefore occur at the same values that encode the Riemann zeros.

The underlying chain is simple enough to state before doing any calculation:

$$\boxed{\text{zeta function}} \longleftrightarrow \boxed{\text{Fourier transform}} \longleftrightarrow \boxed{\text{antenna aperture}} \longleftrightarrow \boxed{\text{radiation-pattern nulls}}.$$

Berry supplied the mathematical antenna proposal; the question pursued here is the next engineering step. Can an explicit, finite electromagnetic structure realize the required aperture strongly enough that the zeros survive a full-wave solution of Maxwell's equations? We first test a 601-element array with prescribed excitations and then replace those hundreds of feeds by a passive slot geometry illuminated by a single plane wave. The latter is the principal realization considered in this article.

3 The van der Pol function

Following van der Pol and Berry, define

$$f(u) = e^{-u/2}\lfloor e^u \rfloor - e^{u/2}, \tag{1}$$

where $\lfloor x \rfloor$ denotes the floor function. Its saw-tooth form is shown in Figure 2. Although elementary in appearance, its Fourier transform carries the zeta function on the critical line.

Using the Fourier convention

$$g(t) = \int_{-\infty}^{\infty} f(u) e^{-itu}\, du, \tag{2}$$

van der Pol's relation gives

$$g(t) = \frac{\zeta\left(\frac{1}{2} + it\right)}{\frac{1}{2} + it}. \tag{3}$$

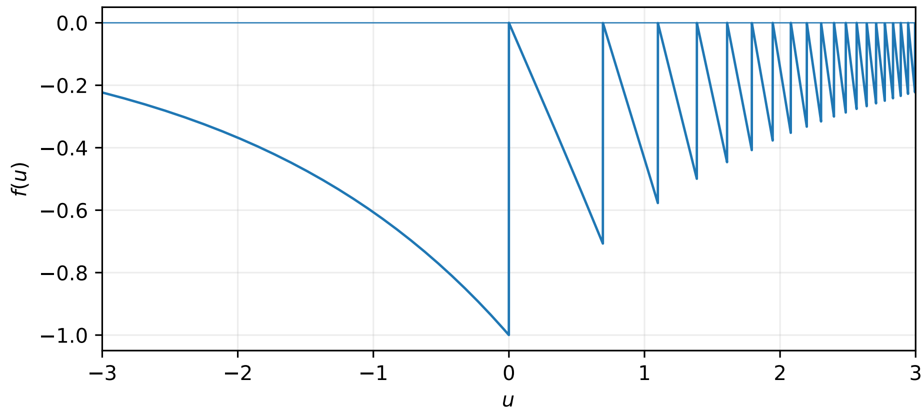

Figure 2: The van der Pol function $f(u)$ in Equation (1). Its elementary saw-tooth form has a Fourier transform proportional to the zeta function on the critical line.

Consequently, whenever $\zeta(\frac{1}{2} + it) = 0$, the transform $g(t)$ also vanishes. The heights t_n of the zeta zeros on the critical line therefore become zeros of a Fourier transform.

This is precisely the form required by antenna theory. If the aperture field of an antenna is proportional to $f(u)$, its far-field pattern can therefore contain the zeros of $g(t)$ and hence the corresponding Riemann zeros.

4 A finite aperture

Equation (2) extends over the whole real line, whereas every physical antenna is finite. We therefore replace it by the truncated transform

$$G(t) = \int_{-u_{\max}}^{u_{\max}} f(u)e^{-itu}\, du. \tag{4}$$

For the numerical calculations used here, u was sampled at intervals $du = 0.01$ and $G(t)$ was compared with the untruncated result for $u_{\max} = 3, 5, 10,$ and 15. For a sampled interval of length $u_{\text{span}} = 2u_{\max}$, the natural discrete Fourier spacing is

$$\Delta t = \frac{2\pi}{u_{\text{span}}}.$$

For $u_{\max} = 3, 5, 10,$ and 15, this gives $\Delta t \approx 1.047, 0.628, 0.314,$ and 0.209, respectively.

As expected, increasing the aperture makes the zero structure sharper. For the antenna simulations, however, physical size matters. The antenna design therefore used $u_{\max} = 3$, accepting some loss of clarity in exchange for a much smaller structure.

5 From Fourier variable to radiation angle

Suppose that successive aperture samples are separated by a physical distance dx, while the corresponding samples of the van der Pol function are separated by du. Thus $u = (du/dx)x$. The phase factor in Equation (2) can then be written

$$e^{-itu} = e^{-it(du/dx)x}.$$

For a one-dimensional aperture, the far-field phase factor in direction θ is $e^{-ikx\sin\theta}$ (up to the choice of angular sign convention), where $k = 2\pi/\lambda$. Matching the two Fourier variables gives

$$t\frac{du}{dx} = k\sin\theta.$$

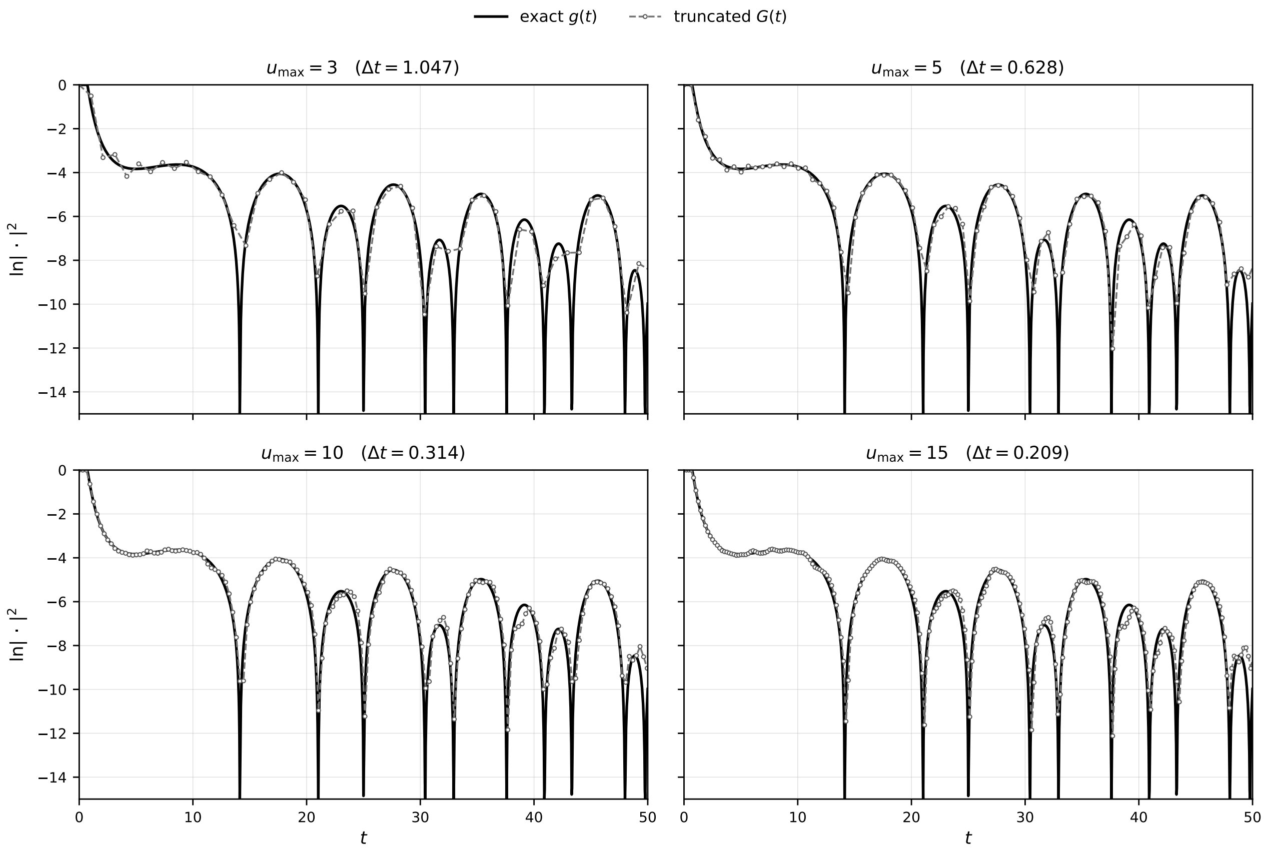

Figure 3: Effect of truncating and sampling the van der Pol aperture. The solid curve is the exact quantity $\ln|g(t)|^2$ from Equation (3); dashed curves with markers show $\ln|G(t)|^2$ computed directly from Equation (4) with $du = 0.01$ at the natural discrete Fourier spacings $\Delta t = 2\pi/(2u_{\max})$. Increasing $u_{\max}$ gives finer Fourier sampling and closer reproduction of the exact zero structure.

Hence a transform zero at $t = t_n$ appears as a radiation null at an angle satisfying

$$\sin\theta_n = \pm\frac{t_n\,du}{k\,dx}. \tag{5}$$

This is the discrete form of Berry's relation $\sin\theta_n = \pm t_n/(kx_0)$, with the scale length $x_0 = dx/du$. The largest accessible value of t is therefore set by the physical sampling ratio kdx/du.

A high operating frequency helps because it reduces the wavelength and hence the overall dimensions of a many-element structure. The simulations described below use 40 GHz.

6 A first realization: 601 dipoles

The first model consists of 601 dipoles separated by 0.8 mm. Their feed voltages follow the sampled van der Pol distribution with $u_{\max} = 3$ and $du = 0.01$. This realization is conceptually direct: prescribe the aperture excitation and ask whether a full electromagnetic model produces the expected zeros.

The fields and radiation patterns were calculated with the CST Time Domain Solver, a full-wave numerical solution of Maxwell's equations. Thus the resulting nulls are not merely the output of a separate Fourier-transform script; they arise from the simulated electromagnetic structure itself. For the slot model described below, the 40 GHz structure was illuminated by a normally incident plane wave propagating in the $+z$ direction, with its electric field parallel to the slot width. The slots were treated as lying in an infinite ground plane, and both the field immediately above the aperture and the resulting far-field radiation pattern were obtained from the full-wave solution.

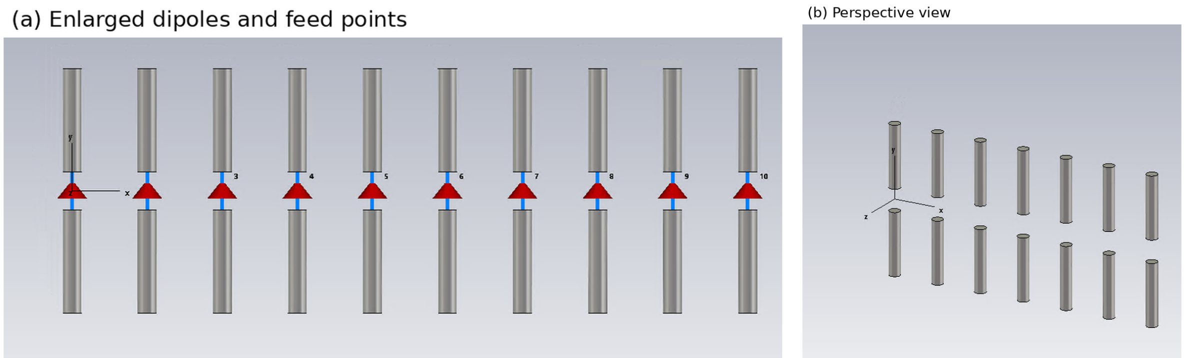

Figure 4: The 601-element 40 GHz dipole-array concept. Panel (a) shows an enlarged section with the feed points; panel (b) gives a perspective view of the element geometry. The excitation amplitudes follow the sampled van der Pol function.

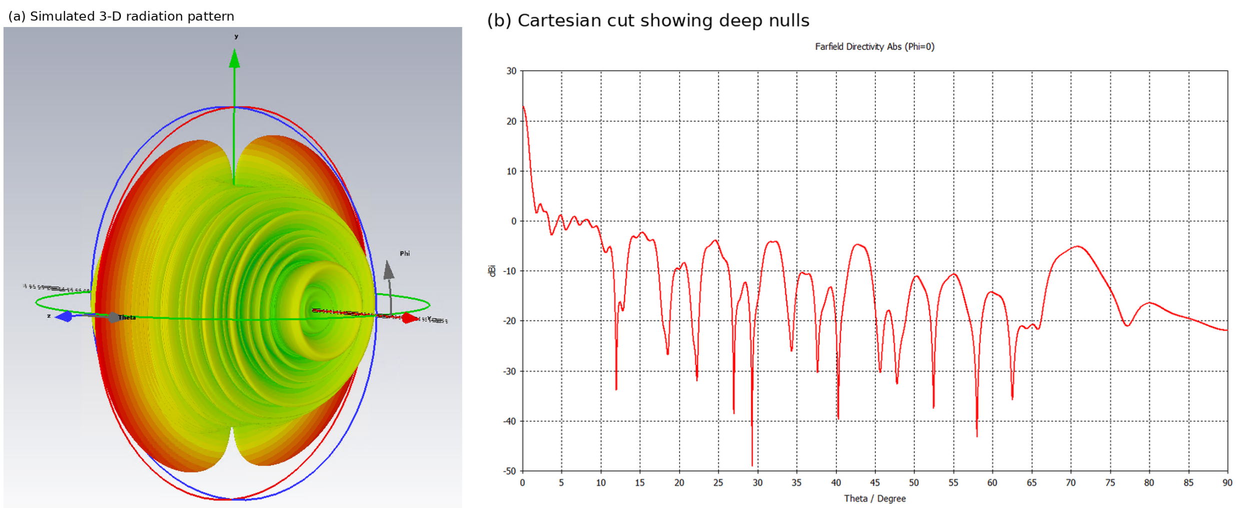

Figure 5: Full-wave CST simulation of the dipole array: (a) the three-dimensional radiation pattern and (b) a Cartesian pattern cut. The deep sidelobe nulls in (b) occur at angles that map to known zeta-zero heights.

The visible range of this model reaches approximately $t = 67$. Converting the simulated null angles by Equation (5) gives zero estimates that typically agree with the known values at approximately the percent level. Table 1 gives a representative sample of the clearly formed nulls.

Table 1: Representative zero heights inferred from the dipole-array nulls, compared with the known values.

n	known t_n	antenna estimate	error (%)
1	14.13	13.95	-1.3
2	21.02	21.36	1.6
3	25.01	25.40	1.6
4	30.42	30.43	0.0
5	32.94	32.82	-0.4
6	37.59	37.85	0.7
7	40.92	41.00	0.2
8	43.33	43.41	0.2

There is, however, an obvious practical weakness. The design assumes that all 601 dipoles can be fed with the required individual amplitudes. The next step was therefore to seek a structure in which the required aperture distribution would arise from geometry rather than from hundreds of separately controlled feeds.

7 A slot array that generates the distribution

A more practical electromagnetic realization is to cut slots in a conducting sheet and illuminate the sheet with a plane electromagnetic wave. The slot dimensions are varied so that the electric field across the aperture approximates the van der Pol distribution.

The simulated design contains 601 slots spaced by 0.8 mm along the long direction. Its overall dimensions are approximately $500\,\mathrm{mm} \times 50\,\mathrm{mm}$. The slots are 5 mm wide, while their lengths were chosen empirically so that the field amplitude sampled above the slots follows the required saw-tooth envelope. In the simulation the aperture field was examined in a plane 0.15 mm above the slots and at the slot centres along the array. A practical version was envisaged as a photo-etched pattern in commercially available 35 μm copper-clad laminate.

This realization is the key physical step in the construction. Instead of specifying 601 independent source voltages, a single incident plane wave illuminates a passive patterned surface. The geometry performs the required amplitude shaping.

8 The Riemann zeros as radiation nulls

The CST radiation pattern of the slot array contains a sequence of sidelobe nulls. When their angles are converted back to the Fourier variable through Equation (5), the inferred values line up with the Riemann zeros. As with the dipole model, the clearly formed nulls typically agree with the known values at approximately the percent level.

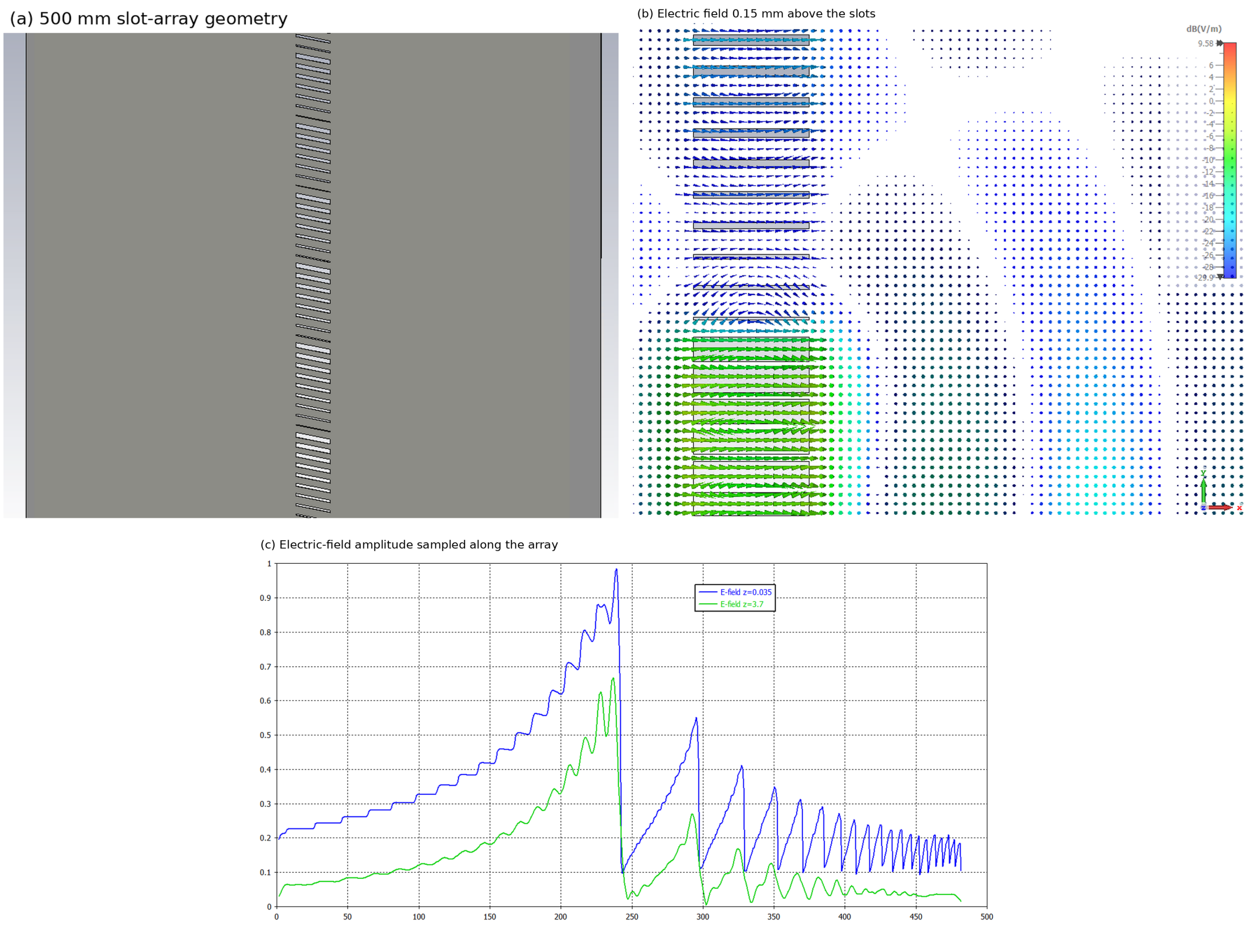

Figure 6: Practical slot-array realization from the CST model: (a) the 500 mm aperture geometry, (b) the simulated electric field 0.15 mm above the slots, and (c) the field amplitude sampled along the array. The varying slot geometry shapes the aperture field toward the van der Pol form.

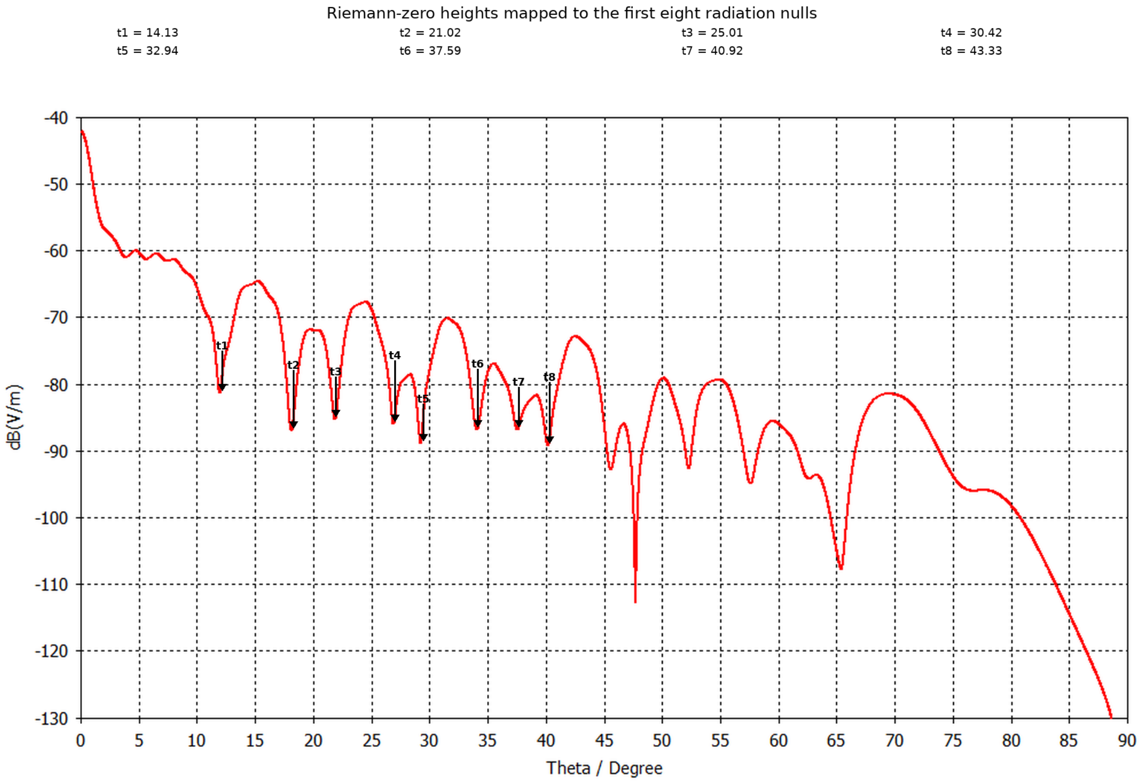

Figure 7: The main simulated result: a Cartesian cut through the slot-array far field. The first eight known zero heights t_n are annotated at the radiation angles predicted by Equation (5); the markers identify the corresponding successive minima of the full-wave result. The red CST trace itself is reproduced unchanged from the simulation; only the mathematical annotations have been added.

This is the main visual result of the article. The correspondence is numerical rather than merely visual: the same numbers that locate zeros of $\zeta(\frac{1}{2} + it)$ locate nulls in the simulated far-field pattern after the simple angular rescaling.

9 How many zeros can be brought into view?

A longer structure increases the accessible Fourier range. An extended design was therefore considered, assembled from three approximately 500 mm sections. The resulting 1500 mm slot array contains 1601 slots with the same 0.8 mm spacing. Its maximum visible height is approximately $t = 208$, so that the angular range encompasses the locations of roughly the first 85 zeta zeros.

The purpose of this extended model is not to catalogue the zeros numerically; those values are already known to far higher precision. Rather, it demonstrates how the mathematical correspondence scales with the physical aperture.

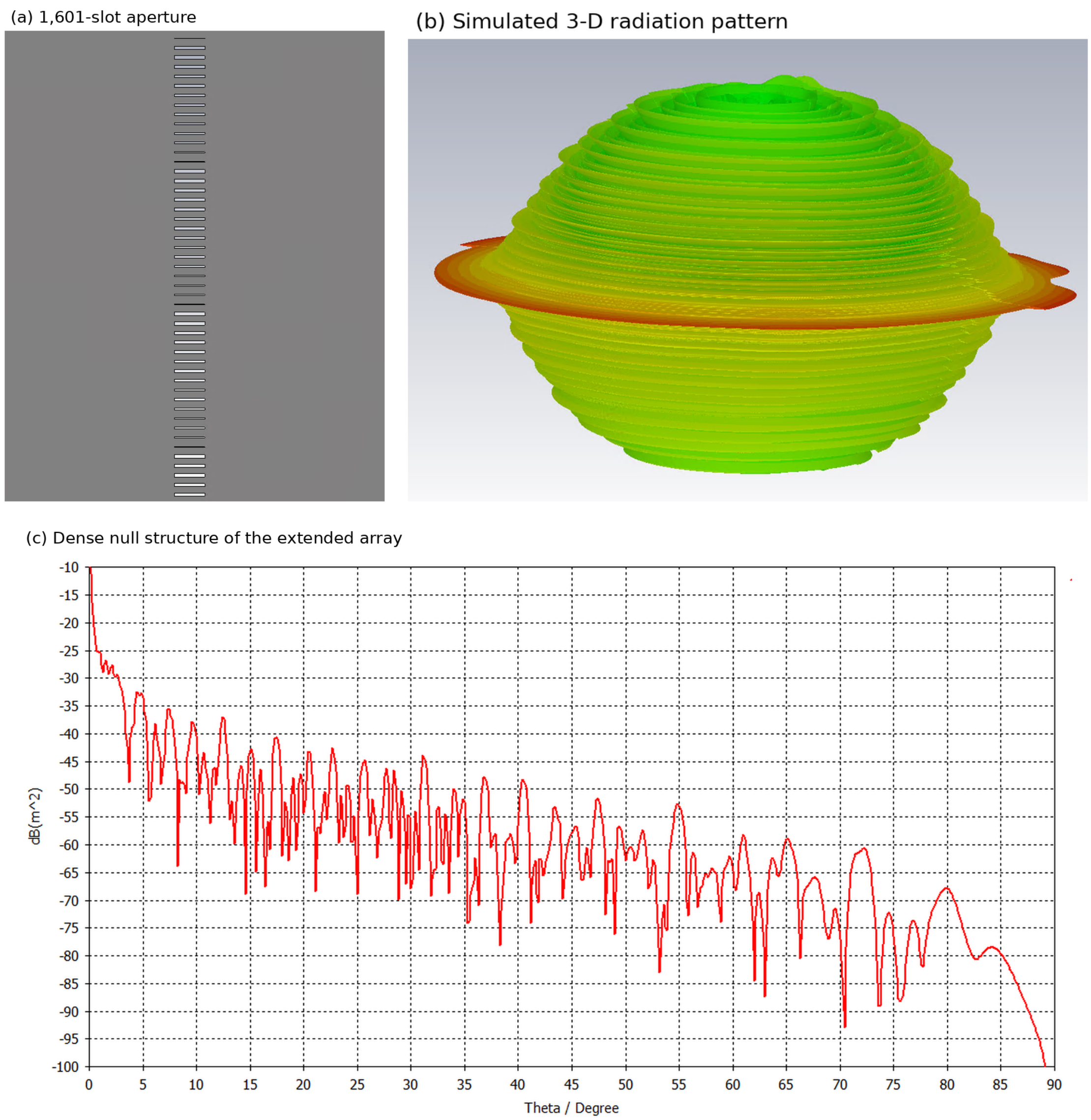

Figure 8: Extended 1601-slot design: (a) the longer aperture geometry, (b) the simulated three-dimensional radiation pattern, and (c) its much denser sequence of nulls. The larger aperture moves the accessible range to about $t = 208$, encompassing the locations of roughly the first 85 zeros.

10 Could the pattern be measured?

The simulations suggest a route to a laboratory visualization, but they also reveal substantial experimental difficulties. A 1.5 m structure could in principle fit within a compact antenna test range, yet the transmitted field through the slots must be observed rather than the reflected field normally used in radar cross-section measurements. The far-field distance is also inconveniently large. One practical alternative would be to sample the transmitted near field and transform the measured data to the far field, although that makes the visualization less direct.

A second difficulty is unwanted transmission and diffraction around the edges of the finite plate, which can fill in deep radiation nulls. A larger conducting surround together with radar-absorbing material near the edges was suggested as a way to reduce this effect.

These limitations are worth retaining because they distinguish a simulated physical realization from a completed experiment. The present claim is therefore deliberately modest: full-wave antenna simulations produce radiation patterns whose nulls reproduce the known Riemann-zero positions.

11 Conclusion

The construction brings together three ideas that normally live in different subjects. Van der Pol supplies a real function whose Fourier transform contains the zeta function on the critical line. Antenna theory supplies a physical Fourier transformer. Full-wave simulation then shows that an aperture designed from the van der Pol function can produce radiation nulls at the corresponding Riemann-zero positions.

The dipole array gives the clearest conceptual realization, while the passive slot array replaces hundreds of prescribed source voltages by a geometrically shaped aperture illuminated by a single plane wave. An extended slot array moves the accessible range to about $t = 208$, encompassing the locations of roughly the first 85 zeros. None of this addresses whether every non-trivial zero lies on the critical line; instead, it offers a striking way of making known zeros visible in an electromagnetic pattern.

Acknowledgments

OpenAI ChatGPT was used in the preparation of this manuscript to assist with editorial revision. The underlying mathematical investigation, antenna designs, electromagnetic simulations, figures and scientific interpretation are the author's work.

References

[1] B. Riemann, Ueber die Anzahl der Primzahlen unter einer gegebenen Gr"osse, *Monatsberichte der K"oniglich Preussischen Akademie der Wissenschaften zu Berlin* (1859), 671–680.

[2] Clay Mathematics Institute, *The Millennium Prize Problems*, 2000.

[3] B. van der Pol, An electro-mechanical investigation of the Riemann zeta function in the critical strip, *Bull. Amer. Math. Soc.* **53** (1947), 976–981.

[4] M. V. Berry, Riemann zeros in radiation patterns, *J. Phys. A: Math. Theor.* **45** (2012), 302001.

[5] M. V. Berry, Riemann zeros in radiation patterns: II. Fourier transforms of zeta, *J. Phys. A: Math. Theor.* **48** (2015), 385203.